



# Pyroelectric and electrocaloric effect of $\langle 111 \rangle$ -oriented 0.9PMN–0.1PT single crystal

Laihui Luo<sup>a,\*</sup>, Hongbing Chen<sup>b</sup>, Yuejin Zhu<sup>a</sup>, Weiping Li<sup>a</sup>, Haosu Luo<sup>c</sup>, Yuepin Zhang<sup>a</sup>

<sup>a</sup> Department of Physics, Ningbo University, Ningbo 315211, China

<sup>b</sup> Institute of Materials Science and Engineering, Ningbo University, Ningbo 315211, China

<sup>c</sup> Shanghai Institute of Ceramics, Chinese Academy of Sciences, Shanghai 200050, China

## ARTICLE INFO

### Article history:

Received 8 March 2011

Received in revised form 28 May 2011

Accepted 30 May 2011

Available online 6 June 2011

### Keywords:

Ferroelectric

Relaxor

Pyroelectric

Electrocaloric

## ABSTRACT

In this paper, the polarization vs. electric field hysteresis loops of  $\langle 111 \rangle$ -oriented 0.9PbMg<sub>1/3</sub>Nb<sub>2/3</sub>O<sub>3</sub>–0.1PbTiO<sub>3</sub> (0.9PMN–0.1PT) single crystal at different temperatures (20–110 °C) were measured. The adiabatic temperature change  $\Delta T$  of  $\langle 111 \rangle$ -oriented 0.9PMN–0.1PT single crystal due to the application or withdraw of electric field were calculated through the thermodynamic relation. The largest temperature change  $\Delta T$  achieves  $\sim 1$  K with only a change of 40 kV/cm electric field, the mechanism of the electrocaloric effect (ECE) is discussed for 0.9PMN–0.1PT crystal. The pyroelectric coefficient of 0.9PMN–0.1PT under bias field was calculated according to the data of hysteresis loop. The result shows that 0.9PMN–0.1PT have large pyroelectric coefficient under bias field, the largest  $(\partial P/\partial T)_E$  value achieves  $-0.5 \mu\text{C}/\text{cm}^2 \text{K}$ .

© 2011 Elsevier B.V. All rights reserved.

## 1. Introduction

During the past decades, many efforts have been put to investigate novel cooling technologies to reduce greenhouse gas and meet new cooling demands in integrated circuits and other field. The electrocaloric effect (ECE) is one of the alternative technologies. ECE is a change in the temperature of dielectrics upon the application or withdraw of an electric field under adiabatic conditions [1]. It attracted much attention in 1960s to 1970s. Bulk ferroelectric ceramic Pb<sub>0.99</sub>Nb<sub>0.02</sub>(Zr<sub>0.75</sub>Sn<sub>0.20</sub>Ti<sub>0.05</sub>)<sub>0.98</sub>O<sub>3</sub> exhibits highest ECE due to the phase transition near its Currie temperature ( $T_c$ ) [2]. Recent years, it has been demonstrated that many ferroelectric films show giant ECE. Mischenko et al. reports that antiferroelectric PbZr<sub>0.95</sub>Ti<sub>0.05</sub>O<sub>3</sub> (PZT) film shows that the largest temperature change  $\Delta T$  achieves 12 K at high temperature 226 °C [1]. Bret Neese et al. reports that relaxor terpolymer P(VDF–TrFE–CFE) also exhibits a giant ECE near room temperature [3]. Ferroelectric relaxor could be attractive for cooling applications due to the occurring of induced paraelectric–ferroelectric phase transition and nanodomain reorientations near its  $T_c$  at a large temperature range. The nonpolar paraelectric to polar ferroelectric transition and nanodomain reorientations can be induced by electric field, and nonpolar paraelectric to polar ferroelectric transition and nanodomain reorientations are disorder–order transition, which will bring entropy change. PbMg<sub>1/3</sub>Nb<sub>2/3</sub>O<sub>3</sub>–PbTiO<sub>3</sub>

(PMN–PT) is a typical ferroelectric relaxor [4,5]. Indeed, PMN–PT ceramic and film have been demonstrated the existence of a giant ECE in PMN–PT system [6–8]. However, the investigated ceramics and films are polycrystalline, which reduces the ECE. The disorder–order transition is easier to occur in PMN–PT single crystal with preferred orientation than in polycrystalline ceramic and film. Therefore, the ECE of PMN–PT single crystal is larger than that of the ceramic and film with the same change of electric field.

PMN–PT single crystal has been proposed for many applications due to its high piezoelectric properties [9,10]. Rhombohedral PMN–PT single crystal have large spontaneous polarization along  $\langle 111 \rangle$  direction. Indeed,  $\langle 111 \rangle$ -oriented PMN–PT single crystal shows pronounced pyroelectricity (converse ECE) under no bias field [11,12], and the pyroelectric coefficient achieves  $0.128 \mu\text{C}/\text{cm}^2 \text{K}$ , which is much larger than that of PMN–PT ceramic and film [13,14]. Large pyroelectricity suggests that ECE of PMN–PT single crystal is strong. Furthermore, disorder–order phase transition in relaxor PMN–PT with low PT content occurs at near room temperature and at a broad temperature range. Therefore, the range of operating temperatures for cooling is wide. However, the ECE of PMN–PT single crystal near room temperature has been investigated little. In this manuscript, we will investigate the ECE and pyroelectric property of  $\langle 111 \rangle$ -oriented 0.91PMN–0.09PT single crystal.

## 2. Experiment and measurement method

PMN–PT single crystal is usually grown by a flux method. However, it is difficult to grow large high-quality crystal due to their complex composition and high

\* Corresponding author. Tel.: +86 574 87600953; fax: +86 574 87600744.  
E-mail addresses: [llhsc@126.com](mailto:llhsc@126.com), [luolaihui@mail.nbu.edu.cn](mailto:luolaihui@mail.nbu.edu.cn) (L. Luo).

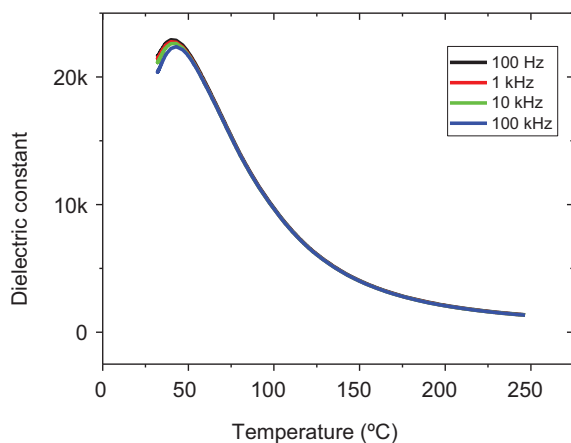


**Fig. 1.** Dielectric constant of the 0.9PMN–0.1PT single crystal as a function of temperature measured with frequencies 100 Hz, 1 kHz, 10 kHz, 100 kHz.

evaporation rate of PbO at high temperature. In this study, we employed the Bridgman technique to grow the crystal. Raw powders of PbO, MgO, Nb<sub>2</sub>O<sub>5</sub>, TiO<sub>2</sub> with high purity were used to synthesize 0.9PMN–0.1PT crystals [15]. To prevent formation of the pyrochlore phase during the crystal growth, the B-site precursor synthesis method was used after the raw powders were mixed completely. The powders were then put into a platinum crucible that was sealed to prevent the evaporation of lead. X-ray diffraction analysis was carried out to confirm the presence of a pure perovskite phase after the crystals were grown.

The as-grown 0.9PMN–0.1PT single crystals were oriented along (111) direction, and then diced into 4 mm × 4 mm × 0.6 mm. Silver paste was pasted on the top and bottom surfaces of the samples and then fired at 650 °C. The dielectric constant  $\epsilon_{33}$  of the (111)-oriented crystals as a function of temperature at 100 Hz, 1 kHz, 10 kHz and 100 kHz were measured using an impedance analyzer (Agilent 4294A). The polarization vs. electric field (*P*–*E*) hysteresis loop at different temperatures (from 20 to 110 °C) was carried out at 1 Hz with the RT Premier II ferroelectric workstation, and the hysteresis loop were made every  $T=5$  °C in the range from 20 to 110 °C.

Reversible electrocaloric temperature change  $\Delta T$  can be calculated by

$$\Delta T = -\frac{T}{C_E} \int_{E_1}^{E_2} \left( \frac{\partial P}{\partial T} \right)_E dE \quad (1)$$

based on the Maxwell relation  $(\partial S/\partial E)_T = (\partial P/\partial T)_E$ . Where  $C_E$  is volumetric specific heat capacity [1]. This formula indicates that the electrocaloric temperature change  $\Delta T$  is dependent on the integrated pyroelectric coefficient. Reversible adiabatic temperature change  $\Delta T$  also can be obtained according to the phenomenological theory and adiabatic temperature change  $\Delta T$  can be obtained using indirect method [16,17]:

$$\Delta T = -\frac{1}{2C_E} \beta T P^2 \quad (2)$$

where  $\beta$  a constant and  $P$  the polarization can be obtained by experiment.

### 3. Results and discussion

Fig. 1 shows the dielectric constant of the 0.9PMN–0.1PT crystals as a function of temperature at 100 Hz, 1 kHz, 10 kHz and 100 kHz. The dielectric constant exhibits obvious frequency dispersion near the dielectric constant maximum. The dielectric constant maximum occurs at 40 °C ( $T_m$ ). 0.9PMN–0.1PT is rhombohedral ferroelectric relaxor at room temperature [18]. On heating above  $T_m$ , the structure of 0.9PMN–0.1PT crystals transforms to a paraelectric cubic state [19,20]. The ferroelectric–paraelectric transition occurs at a broad temperature range near  $T_m$  due to microscopic inhomogeneities, so there are still nanodomains in 0.9PMN–0.1PT crystals even at above  $T_m$ . The ferroelectric–paraelectric transition is first-order phase transition. The phase transition induces a large polarization change. The large ECE can be obtained in a broad temperature range due to the relaxor phase transformation.

Fig. 2 shows several typical *P*–*E* hysteresis loops of the 0.9PMN–0.1PT crystal at different temperatures. The largest field applied to the 0.9PMN–0.1PT is 40 kV/cm; larger field will break down the sample. The figure shows that the polarization of the crystal decreases with the temperature. 0.9PMN–0.1PT crystals are

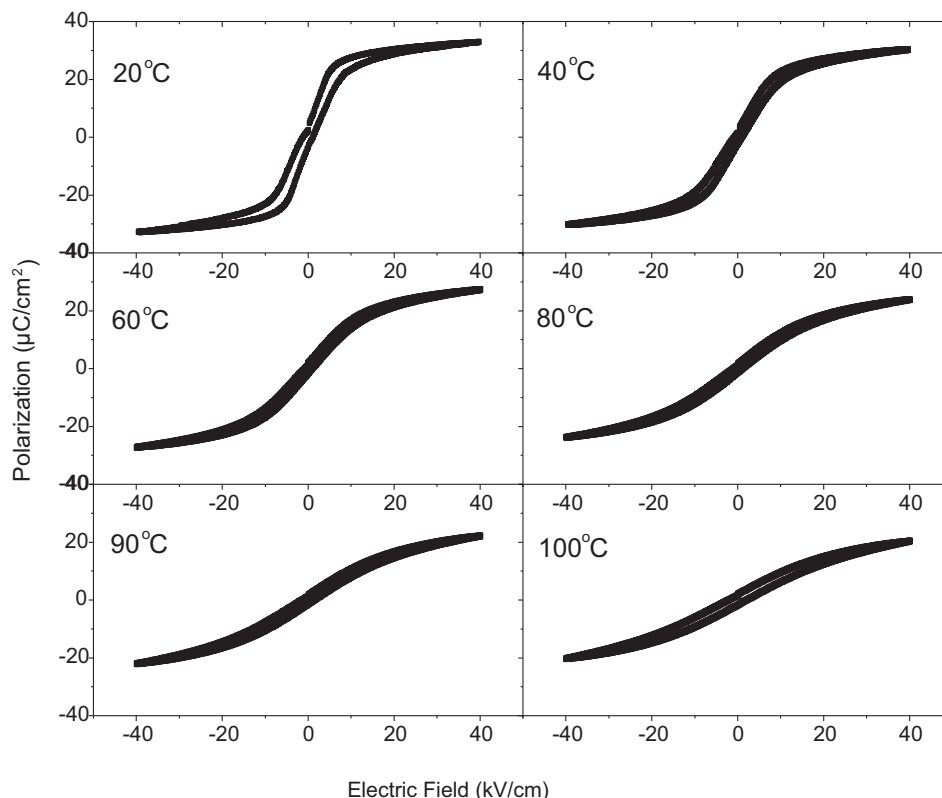


**Fig. 2.** Polarization vs. electric field hysteresis loops of 0.9PMN–0.1PT single crystal at different temperatures.

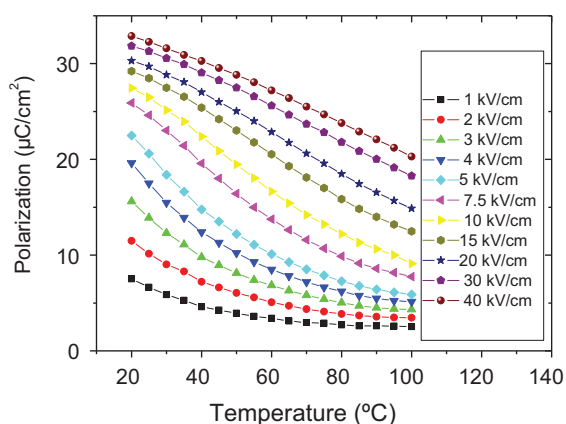


Fig. 3. Polarization as a function of temperature under different electric fields.

paraelectric phase above  $T_m$ , however, the polarization is still large even the temperature reaching  $100^\circ\text{C}$ . The large polarization at above  $T_m$  is due to the existence of nanodomain since microscopic inhomogeneities in 0.9PMN–0.1PT crystals, and ferroelectric phase also can be induced by electric field. The area of the hysteresis loops is a little, which indicates the energy loss is a little during the operation of application and withdraw of electric field.

Fig. 3 shows the polarization as a function of temperature under different fields for 0.9PMN–0.1PT, which is extracted from the upper branch of the hysteresis loop. The curve was fitted with a fourth order polynomials, and the value of  $(\partial P/\partial T)_E$  was calculated from the derivation of the fitted polynomials. From Fig. 3, we know that  $(\partial P/\partial T)_E$  value varies with the temperature and electric field. Large  $(\partial P/\partial T)_E$  value will result in large  $\Delta T$  value. The largest  $(\partial P/\partial T)_E$  value achieves  $-0.5 \mu\text{C}/\text{cm}^2 \text{K}$  under zero bias field at room temperature, which is much larger than that of commonly used pyroelectric material barium strontium titanate (BST) ( $\partial P/\partial T = 4.1 \times 10^{-2} \mu\text{C}/\text{cm}^2 \text{K}$ ) [21]. At  $E > 20 \text{ kV}/\text{cm}$ , the polarization is almost linear with temperature. From the slope of the curves, we know that the  $(\partial P/\partial T)_E$  value varies a little with the temperature at high field. The  $(\partial P/\partial T)_E$  value of 0.9PMN–0.1PT is very high, compared with those of other ferroelectrics with high ECE, such as PMN–PT film, PZT film, terpolymer P(VDF–TrFE–CFE) film. Large  $(\partial P/\partial T)_E$  value indicates that 0.9PMN–0.1PT is an excellent pyroelectric material under bias field. Fig. 4 exhibits several  $(\partial P/\partial T)_E$  values as a function of temperature under different bias fields,

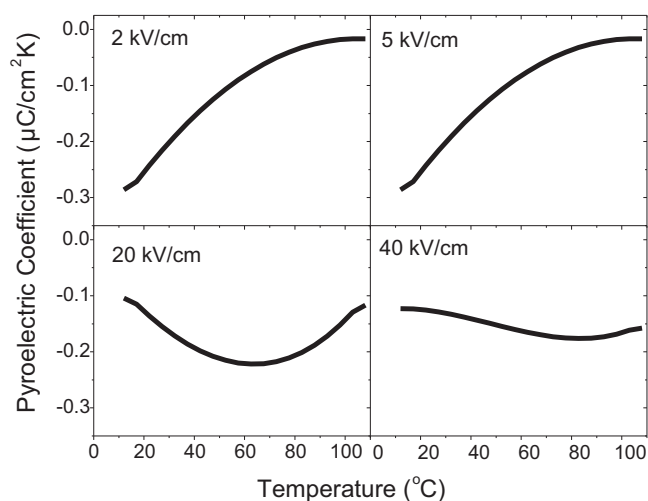


Fig. 4. Pyroelectric coefficient as a function of temperature under different electric fields.

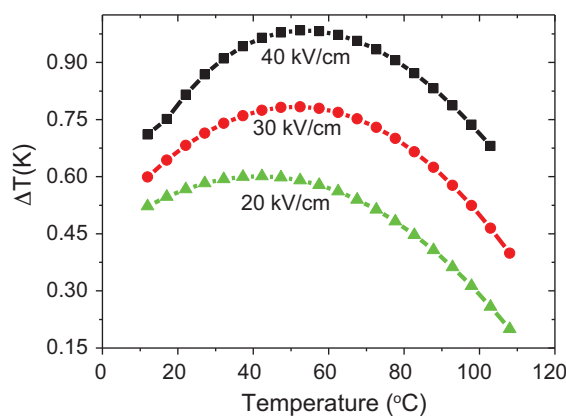


Fig. 5. Adiabatic temperature change  $\Delta T$  due to different change of electric field.

which are obtained by calculating the slope of the curve as presented in Fig. 3. Fig. 4 shows that the highest  $(\partial P/\partial T)_E$  value in the curve moves to higher temperature and decreases as the  $E$  field bias increases, which indicates that the 0.9PMN–0.1PT is easy for depolarization under low field and large electric field change is necessary to obtain large ECE in 0.9PMN–0.1PT at high constant field.

The reversible adiabatic temperature change  $\Delta T$  due to an application or withdraw of electric field from  $E_1$  to  $E_2$  can be determined according to formula (1). Reversible adiabatic temperature change  $\Delta T$  also can be measured by direct method using differential scanning calorimetry (DSC) [22,23]. There is a little difference between the  $\Delta T$  value calculated using the Maxwell relationships and the  $\Delta T$  value measured by DSC [24]. From formula (1), it is obvious that the maximum value of adiabatic temperature change  $\Delta T$  of a dielectric material is mainly dependent on the value of breakdown field  $E_2$  and pyroelectric coefficient  $(\partial P/\partial T)_E$  at constant electric field. It is difficult to apply a large field to bulk materials without causing electrical breakdown. A large change of electric field leads to a large ECE for the dielectrics. The defects in the 0.9PMN–0.1PT crystal reduces the breakdown field greatly, there are lots of defects such as oxygen vacancies and dislocations in the as-grown crystal. The quality of the crystal should be improved further to enhance the breakdown field. Thinning the sample by chemical etching and mechanical grinding is also a feasible method to improve the dielectric breakdown field.

At the temperature range from room temperature to  $110^\circ\text{C}$ , the volumetric specific heat capacity  $C_E$  is considered as a constant, and  $C_E = \rho c$ , where  $c$  is heat capacity per unit mass, it is  $\sim 330 \text{ J}/\text{kg K}$ , which is extracted from the work of Tang et al. [25]. The density  $\rho$  of 0.9PMN–0.1PT is  $8.1 \times 10^3 \text{ kg}/\text{m}^3$ , and the value is measured by Archimedes method. When calculating the adiabatic temperature change  $\Delta T$ , the data  $E_1 = 0 \text{ kV}/\text{cm}$ ,  $E_2 = 40 \text{ kV}/\text{cm}$  are used. Fig. 5 shows the adiabatic temperature change  $\Delta T$  as a function of temperature with different change of electric field, which are calculated according to formula (1). The largest temperature change  $\Delta T$  occurs at above  $T_m$ .

The largest  $\Delta T$  achieves  $\sim 1 \text{ K}$  with only a change of  $40 \text{ kV}/\text{cm}$  electric field. The temperature change  $\Delta T$  is relatively low, compared with that of polycrystalline film [3,7,8].  $\Delta T$  value of PMN–PT achieves  $12 \text{ K}$  with a large electric field change of  $895 \text{ kV}/\text{cm}$ , and the value is also  $12 \text{ K}$  in a even larger electric field  $2090 \text{ kV}/\text{cm}$  for relaxor terpolymer P(VDF–TrFE–CFE). The value is higher than that of PMN–PT ceramic [26]. The  $\Delta T$  of PMN–PT ceramic is  $0.558 \text{ K}$  with a large electric field change of  $24 \text{ kV}/\text{cm}$  ( $0.023 \text{ K cm}/\text{kV}$ ). Comparing the ECE of these materials, it can be seen that PMN–PT crystal has the largest ECE per unit applied electric field. The temperature change per unit applied electric field is  $0.025 \text{ K cm}/\text{kV}$  for PMN–PT crystal,  $0.013 \text{ K cm}/\text{kV}$  for PMN–PT thin film,  $0.0057 \text{ K cm}/\text{kV}$  for

P(VDF-TrFE-CFE) film and 0.023 K cm/kV for bulk PMN-PT ceramic. The reason resulting in the relatively low  $\Delta T$  for bulk 0.9PMN-0.1PT single crystal and ceramic is the much smaller breakdown field than film.  $\Delta T$  varies mildly with the temperature, which indicates that ECE can be obtained in a broad temperature range. Fig. 5 also shows that  $\Delta T$  value is dependent on the change of electric field greatly. If the breakdown field is improved, the 0.9PMN-0.1PT crystal should be an excellent candidate for application in both room cooling equipment and pyroelectric devices.

#### 4. Conclusion

In this work, we have investigated the electrocaloric effect of (111)-oriented 0.9PMN-0.1PT single crystal through the thermodynamic relation. The largest adiabatic temperature change  $\Delta T$  occurs at above  $T_m$  of 0.9PMN-0.1PT single crystal. The largest  $\Delta T$  achieves  $\sim 1$  K with only a change of 40 kV/cm electric field and the temperature change per unit applied electric field reaches 0.025 K cm/kV. The value of  $\Delta T$  value is dependent on the change of electric field greatly. Further larger ECE is limited by the breakdown field of the 0.9PMN-0.1PT single crystal. The 0.9PMN-0.1PT single crystal have large pyroelectric coefficient under bias field, the largest  $(\partial P/\partial T)_E$  value achieves  $-0.5 \mu\text{C}/\text{cm}^2 \text{K}$ , which indicates 0.9PMN-0.1PT single crystal is an excellent pyroelectric material.

#### Acknowledgments

This work was supported by National Natural Science Foundation of China (51002082, 11004113, 60807036), Natural Science Foundation of Zhejiang Province (Y4090429), Natural Science Foundation of Ningbo (2009A610103, 2009G610012), The Prior Project In Key Science & Technology Program of Zhejiang Province

(2009C11144, 2008C21069) and K. C. Wong Magna Foundation in Ningbo University (xkl09063, XYL10012).

#### References

- [1] A.S. Mischenko, Q. Zhang, J.F. Scott, R.W. Whatmore, N.D. Mathur, *Science* 311 (2006) 1270–1271.
- [2] B.A. Tuttle, D.A. Payne, *Ferroelectrics*, 1981, pp. 603–606 <http://www.informaworld.com/smpp/title~db=all~content=t713617887~tab=issueslist~branches=37-v3737>.
- [3] B. Neese, B. Chu, S. Lu, Y. Wang, E. Furman, Q.M. Zhang, *Science* 321 (2008) 821–823.
- [4] L.B. Kong, J. Ma, W. Zhu, O.K. Tan, *J. Alloy Compd.* 336 (2002) 242–246.
- [5] D. Lin, Z. Li, F. Lia, Z. Xua, X. Yao, *J. Alloy Compd.* 489 (2010) 115–118.
- [6] S. Liu, Y. Li, *Mater. Sci. Eng. B* 113 (2004) 46–49.
- [7] T.M. Correia, J.S. Young, R.W. Whatmore, J.F. Scott, N.D. Mathur, *Appl. Phys. Lett.* 95 (2009) 182904.
- [8] A.S. Mischenko, Q. Zhang, R.W. Whatmore, J.F. Scott, N.D. Mathur, *Appl. Phys. Lett.* 89 (2006) 242912.
- [9] S.E. Park, T.R. Shrout, *J. Appl. Phys.* 82 (1997) 1804.
- [10] L. Luo, H. Wang, Y. Tang, X. Zhao, Z. Feng, et al., *J. Appl. Phys.* 99 (2006) 024104.
- [11] Y. Tang, L. Luo, Y. Jia, H. Luo, et al., *Appl. Phys. Lett.* 89 (2006) 162906.
- [12] Y. Tang, X. Zhao, X. Feng, W. Jin, H. Luo, *Appl. Phys. Lett.* 86 (2005) 082901.
- [13] W. Cho, T.R. Shrout, J. Jang, A.S. Bhalla, *Ferroelectrics* 100 (1989) 29–38.
- [14] J. Wang, K.H. Wong, H.L.W. Chan, C.L. Choy, *Appl. Phys. A Mater.* 79 (2004) 551–556.
- [15] H. Luo, G. Xu, H. Xu, P. Wang, Z. Yin, *Jpn. J. Appl. Phys.* 39 (2000) 5581–5585.
- [16] S.G. Lu, Q.M. Zhang, Z. Kutnjak, et al., *Appl. Phys. Lett.* 97 (2010) 162904.
- [17] S. Lu, Q. Zhang, *Adv. Mater.* 21 (2009) 1983–1987.
- [18] D. Viehland, J.F. Li, *J. Appl. Phys.* 89 (2001) 1826.
- [19] Z.G. Ye, B. Noheda, M. Dong, D. Cox, G. Shirane, *Phys. Rev. B* 64 (2001) 184114.
- [20] D. Zekria, V.A. Shuvaeva, A.M. Glazer, *J. Phys.: Condens. Matter* 17 (2005) 1593.
- [21] J. Cheng, J. Tang, J. Chu, A. Zhang, *Appl. Phys. Lett.* 77 (2000) 1035.
- [22] D. Guyomar, G. Sebald, B. Guiffard, L. Seveyrat, *J. Phys. D: Appl. Phys.* 39 (2006) 4491–4496.
- [23] S. Kar-Narayan, N.D. Mathur, *J. Phys. D: Appl. Phys.* 43 (2010) 032002.
- [24] G. Sebald, S. Pruvost, L. Seveyrat, L. Lebrun, D. Guyomar, B. Guiffard, *J. Eur. Ceram. Soc.* 27 (2007) 4021–4024.
- [25] Y. Tang, X. Wan, X. Zhao, X. Pan, D. Lin, H. Luo, J. Sun, et al., *J. Appl. Phys.* 98 (2005) 084104.
- [26] J. Hagberg, A. Uusimäki, H. Jantunen, *Appl. Phys. Lett.* 92 (2008) 132909.